

## **Paper 4**

# **Venturi Meters in Wet Gas Flow**

*D. G. Stewart, D. Hodges and G. Brown,  
National Engineering Laboratory, UK*

# **VENTURI METERS IN WET GAS FLOW**

**David G. Stewart, David Hodges, Gregor J Brown, NEL**

---

## **1 Introduction**

Multiphase metering is becoming increasingly important in the development of marginal oil and gas fields. Many of these fields are only economically viable if they can be tied back to existing platform infrastructure, reducing the capital expenditure required by significant margins. In such cases, several fields are often tied back to common facilities requiring each unprocessed stream to be metered before co-mingling.

Multiphase metering is also a valuable technology in well management, providing on-line information on the production flow; and in well testing, reducing the capital expenditure required to investigate potential new wells.

Wet gas metering is at the high gas fraction end of multiphase metering, typically with a gas volume fraction (GVF) above 90%, and mostly above 95%. Standard multiphase meters cannot operate satisfactorily in such conditions. The development of Wet Gas Meters is therefore a key requirement of the oil and gas industry.

There are two principal approaches to wet gas metering. The first is to use a dedicated wet gas meter which has been designed to measure the flow rates of both the liquid and gas phases. The second is to use a standard dry gas meter and apply corrections to the measurements based on knowledge of how the meter in question is affected by the presence of a liquid phase in the gas stream. The second method requires prior knowledge of the liquid flow to correct for the gas flow.

Obviously the first method is desirable from the point of view of continuous measurement and well management, however if the liquid flow is known to remain reasonably constant, or change slowly then the second method can be used, subject to a suitable means of determining the liquid flow being available.

The work presented in this paper is relevant to both methods. Using the second method with a Venturi meter requires a detailed knowledge of the performance of Venturi meters in wet gas flows. The data contained in this paper offers a significant contribution to this knowledge. The data may also prove useful in the development of commercial Wet Gas Meters based on Venturis.

## **2 Venturi meters in wet gas flow**

Venturi meters have become increasingly popular in the measurement of wet gas flows, particularly for allocation purposes and well management. Venturi meters are less susceptible to damage from liquid slugs than orifice plates and due to the convergent inlet section, the hold up of liquid is less pronounced than in an orifice plate.

When Venturi meters, or any other differential pressure meters, are used in wet gas flow the measured differential pressure is higher than it would be if the gas phase were flowing alone. It is believed that this is caused by energy losses at the gas liquid interface(s) as the gas drives the liquid along the pipe. The exact amount of additional pressure loss will depend on several parameters, including the amount of liquid present, pressure, gas velocity, liquid density, viscosity

and surface tension, and the flow regime in the pipe (stratified or annular mist). This additional pressure drop produces an overreading in the apparent gas mass flowrate, compared with what would be measured without any liquid present. This difference must be corrected for using some form of overreading correlation.

Several correlations have been proposed over the years, e.g. Murdock [1], Chisholm [2,3], Lin [4], de Leeuw [5], and Steven [6]. Steven gives a good background on these correlations [6]. The Murdock correction is the most well known of these, and is expressed as:

$$m_{g(actual)} = \frac{m_{g(tp)}}{1 + 1.26X} \quad (1)$$

where  $m_{g(actual)}$  is the corrected gas mass flowrate,  $m_{g(tp)}$  is the apparent gas mass flowrate determined from the two-phase measured differential pressure and  $X$  is the “modified” Lockhart-Martinelli, defined as:

$$X = \frac{m_l}{m_g} \sqrt{\frac{\rho_g}{\rho_l}} \quad (2)$$

where  $m_l$  and  $m_g$  are the liquid and gas mass flowrates, and  $\rho_l$  and  $\rho_g$  are the liquid and gas densities. The apparent gas mass flowrate is given by:

$$m_{g(tp)} = CE\varepsilon A_d \sqrt{2\rho_g \Delta p_{(tp)}} \quad (3)$$

where  $E$  is the velocity of approach factor  $(1/\sqrt{1-\beta^4})$ ,  $\varepsilon$  is the gas expansibility factor,  $A_d$  is the throat area and  $\Delta p_{(tp)}$  is the measured two-phase differential pressure.

Murdock’s original correction factor was based on several sets of orifice plate data from different sources. de Leeuw [5] and Steven [6] both carried out wet gas tests using Venturi meters and found that both the Murdock and the Chisholm correction factors were not suitable for Venturis. At present the only way to ensure an accurate correction for wet gas operation is to test a meter prior to installation in a wet gas test facility. Whilst de Leeuw and Steven both published improved correction factors based on their own data, it is clear that further work is required in this area to provide a larger, more reliable data set on which to base further improved correction factors. This paper presents results from wet gas tests at NEL, which expand the available data set considerably.

### 3 NEL High-Pressure Wet Gas Test Facility

This facility has been operational since 1999, and has been heavily used for research, testing and calibration work since. The facility is a recirculating loop based around a 12m<sup>3</sup> gas/liquid separator. The test section is nominally four or six inch, but sizes from 2 inch to 8 inch can be accommodated. The fluids used are nitrogen (density range 2 to 70 kg/m<sup>3</sup>) and a kerosene substitute (Exxsol D80; approximate density of 800 kg/m<sup>3</sup>). These fluids were deemed suitable for simulation of gas/condensate streams, taking into account the desire for accurate reference measurements and the safety requirements regarding volatile hydrocarbons usage in the laboratory at NEL. The facility operates at ambient temperatures of approximately 20°C at pressures up to 62 barg.

The gas is drawn from the top of the separator and driven round the loop by a 200 kW gas blower up to a maximum dry gas flowrate of 1200 m<sup>3</sup>/hr. Liquid is injected through an injection spool over 50D upstream of the test section. The gas and liquid temperatures are both controlled with heat exchangers to maintain equal temperatures in the test section. The gas and liquid reference flowrates are measured using traceable calibrated reference turbines. The expanded uncertainty on the gas mass flowrate is  $\pm 0.35\%$  and  $\pm 0.15\%$  for the liquid mass flowrate (both at the 95% confidence level). All temperature and pressure measurements are taken using traceable calibrated instrumentation. A modified subsea video camera can be used to monitor the two-phase flow in the test section. The camera view allows the transition from stratified flow to annular/mist flow to be observed.

#### 4 Test Program and Results

Three 4-inch Venturi meters,  $\beta = 0.4, 0.6$  and  $0.75$ , were tested in wet gas at three test pressures, 15 bar, 30 bar and 60 bar. The different  $\beta$  values would show whether or not the overreading was dependent on  $\beta$ . All previous wet gas Venturi tests have only been carried out with one meter and hence were unable to determine a  $\beta$  dependence or otherwise. The three test pressures would allow the effect of the gas density to be investigated. The meters were tested across a range of gas and liquid flowrates, to investigate the effect of liquid content and gas velocity. These are shown in Table 1, expressed by the gas densimetric Froude number,  $Fr_g$ , and  $X$ . The gas Froude number is a dimensionless number defined as:

$$Fr_g = \frac{v_{sg}}{\sqrt{gD}} \sqrt{\frac{\rho_g}{\rho_l - \rho_g}} \quad (4)$$

where  $v_{sg}$  is the superficial gas velocity,  $g$  is the gravitational constant and  $D$  is the upstream pipe diameter.

**Table 1. Envelope for wet gas Venturi tests.**

| $\beta$ | Pressure (bar) | $Fr_g$    |
|---------|----------------|-----------|
| 0.4     | 15             | 0.5 – 2.5 |
|         | 30             | 1.0 – 3.0 |
|         | 60             | 1.5 – 3.5 |
| 0.6     | 15             | 1.5 – 3.5 |
|         | 30             | 1.5 – 4.5 |
|         | 60             | 1.5 – 5.5 |
| 0.75    | 15             | 1.5 – 3.5 |
|         | 30             | 1.5 – 4.5 |
|         | 60             | 1.5 – 5.5 |

The maximum Lockhart-Martinelli value,  $X$ , was 0.3 where achievable, depending on the gas Froude number, pressure and  $\beta$  value.

##### 4.1 Calculation of overreading

Each Venturi was calibrated in dry gas at each test pressure prior to the respective wet gas test matrix, to establish a dry gas baseline against which the wet gas results can be compared. When analysing the subsequent wet gas data, the meter overreading can be calculated from:

$$O.R. = \sqrt{\frac{\Delta_{(tp)}}{\Delta_g}} \quad (5)$$

where  $\Delta_g$  is the dry gas differential pressure that would be measured had the gas been flowing alone. This is calculated using the dry gas calibration data and measured reference gas flowrate and density:

$$\sqrt{\Delta_g} = \frac{K_{g,ref}}{K_g} \sqrt{2\rho} \quad (6)$$

where  $K_g$  is the dry gas flow coefficient, defined as:

$$K_g = \varepsilon = f(\text{Re}_{g,ref}) \quad (7)$$

where  $\text{Re}_{g,ref}$  is the reference gas Reynolds number.

## 4.2 Discussion of results

The overreading plots from the  $\beta = 0.4$  Venturi are shown in Figs. 1 to 3, for the 15 bar, 30 bar, and 60 bar tests. Figs. 4 to 6 and Figs. 7 to 9 show the overreading plots for the  $\beta = 0.6$  Venturi and the  $\beta = 0.75$  Venturi respectively, in the same pressure order as the  $\beta = 0.4$  results. The data is presented as meter overreading vs.  $X$ , and plotted in different series based on  $Fr_g$ .

It is clear from all the results that the overreading increases with increasing  $X$ , as expected. It is also clear that all the data sets show a degree of curvature, particularly at lower values of  $X$ , i.e. at  $X < 0.1$ . The curvature is most pronounced at lower pressures, as shown in Figs. 1, 4 and 7.

These results also show that the gas pressure (or density) has a significant effect on the overreading. It can be seen from any of the data sets that the overreading decreases with increasing pressure. For example, Figs 5 and 6 both show data for the beta 0.6 Venturi, at 30 bar and 60 bar respectively. At 30 bar the overreading at  $X = 0.3$  and  $Fr_g = 3.5$  is approximately 1.65, whilst at 60 bar the overreading of approximately 1.52 for the same  $X$  and  $Fr_g$ . This is in agreement with the findings of both de Leeuw [5] and Steven [6].

Another trend that is clearly evident from Figs. 1 to 9 is that the overreading is dependent on the gas Froude number,  $Fr_g$  (or gas velocity). In all cases, the overreading increases with increasing  $Fr_g$ . This again is in agreement with the findings of de Leeuw and Steven. There is clear separation between the data sets at different values of  $Fr_g$  at all pressures. This effect is thought to be due to the nature of the flow regime in the pipe. Fig. 10, which shows a reproduction of a Shell two-phase flow regime map, taken from [4], helps to illustrate this point. At lower gas velocities the flow regime is stratified, with most or all of the liquid running along the bottom of the pipe. The gas/liquid interface is relatively low at these conditions. As the gas velocity increases, more of the liquid becomes entrained in the gas and around the pipe wall, increasing the overall area of the gas/liquid interface and consequently the energy loss as the gas drives the liquid. This results in an increase in the meter overreading. It would be expected, therefore, that a limit would be reached at which increasing gas velocity has a diminishing effect on the overreading as by this point all the liquid will be fully entrained in the gas stream as small droplets travelling closer to the gas velocity. Evidence of this can be seen from the data presented, particularly for the  $\beta = 0.6$  and  $\beta = 0.75$  meters, where the highest values of  $Fr_g$  were reached. Figs. 4 to 9 all show the curves "bunching up" at higher values of  $Fr_g$ , i.e. the effect of increasing  $Fr_g$  decreases at higher values of  $Fr_g$ .

As stated earlier, no previous wet gas Venturi tests had been carried out using Venturis with different  $\beta$  values. In this work the three Venturis allow the dependence on  $\beta$  to be investigated. Figs. 11 to 16 show the overreading plots for two values of  $Fr_g$  at each of the three pressures, with the data from each meter plotted together. It is clear from these graphs that the  $\beta$  value does in fact have a significant effect on the meter overreading. In all cases, the overreading decreases with increasing  $\beta$  value. Analysis of Figs. 11, 13 and 15 (where all three  $\beta$  values are plotted) appears to show that the spread in the overreading curves at different  $\beta$  values reduces with increasing pressure. Figs. 12, 14 and 16 also appear to show this, although only for two values of  $\beta$ . Also, analysis of the two graphs at each pressure (i.e. Figs. 11 and 12, 13 and 14, 15 and 16) shows that the spread appears to increase at higher values of  $Fr_g$ . This is based on examination of the difference between the  $\beta = 0.6$  and  $\beta = 0.75$  data at the two values of  $Fr_g$  shown for each pressure. This dependence on  $\beta$  introduces yet another variable into the picture when trying to predict the overreading in wet gas Venturis. This could have a significant impact on the design of Venturi-based wet gas meters, as if a manufacturer wanted to offer the meter with different  $\beta$  values, then the initial product development test program would have to address this fact.

### 4.3 Comparison with previous work

As stated previously there have been several works on wet gas measurement in the past. The most significant of these in terms of impact on the knowledge of the topic in general was that of Murdock [1]. Murdock developed a correlation for two phase flow based on several sets of data generated using orifice plates across a wide range of conditions. Steven [6] gives a detailed description of this work and the correlation derived. However, as this work is based exclusively on orifice plates, and de Leeuw [5] and Steven [6] have shown it to be of little use when considering wet gas Venturis, no comparison is made with Murdock's work.

Chisholm [2] later published another correlation, again based on orifice plate data. Significantly, however, Chisholm subsequently published a research note [3] that modified his correlation to include a dependence on the gas pressure.

The most significant advance since Murdock and Chisholm comes from the work of de Leeuw [5], as this work was the first to be based exclusively on wet gas Venturi data. de Leeuw confirmed that the overreading was dependent on the gas pressure (density), and that the overreading decreased with increasing pressure. The most significant aspect of de Leeuw's work was the discovery that the overreading was also dependent on the gas velocity or Froude number,  $Fr_g$ . de Leeuw took this into account when developing his correlation, which is expressed as:

$$\sqrt{\frac{\Delta_{(tp)}}{\Delta_g}} = \sqrt{1 + X + X^2} \quad (8)$$

where

$$= \left( \frac{\rho_l}{\rho_g} \right)^n + \left( \frac{\rho_g}{\rho_l} \right)^n \text{ and}$$

$$n = 0.606 \left( 1 - e^{-0.746 Fr_g} \right) \quad \text{for } Fr_g \geq 1.5$$

$$n = 0.41 \quad \text{for } 0.5 \leq Fr_g \leq 1.5$$

de Leeuw's work used a 4-inch  $\beta = 0.4$  Venturi using nitrogen and diesel oil as the test fluids. The range of test conditions is shown as a dotted envelope on the Shell flow map in Fig. 10.

Steven's work [6] used tested a 6-inch  $\beta = 0.55$  Venturi. These tests were one of the first wet gas tests carried out on the NEL Wet Gas Facility following commissioning in 1999. This facility has been modified since to increase the available gas and liquid flow slightly from what was available for Steven [6]. Steven tested this Venturi at 20 bar, 40 bar and 60 bar at gas flowrates between 400 m<sup>3</sup>/hr and 1000 m<sup>3</sup>/hr, with liquid volume fractions between 0.1% and 5%. Steven's results confirmed de Leeuw's findings that the overreading was dependent on  $Fr_g$  as well as pressure. Steven undertook a detailed analysis of all previous correlations and their suitability for predicting the overreadings obtained in his work. Following this, he then presented a new empirical correlation based on his own results:

$$\sqrt{\frac{\Delta_{(tp)}}{\Delta_g}} = \frac{1 + \frac{X + B}{1 + X + \frac{C}{D}}}{g} \quad (9)$$

where  $A$ ,  $B$ ,  $C$  and  $D$  are pressure dependent empirical constants:

$$A = 4.777285e-3 p^2 - 0.5242366 p + 17.11304$$

$$B = 1.233263e-4 p^2 - 0.0113753 p + 0.203878$$

$$C = 3.354571e-3 p^2 - 0.3673168 p + 11.02978$$

$$D = 1.149112e-4 p^2 - 0.0104724 p + 0.177765$$

where  $p$  is the pressure in barg.

Examples of how both de Leeuw's and Steven's correlations compare with the data presented in this paper are shown in Figs. 17 to 20. Fig. 17 shows the comparison for the  $\beta = 0.4$  Venturi at 15 bar. It can be seen that de Leeuw's correlation fits reasonably well, particularly at the higher Froude number,  $Fr_g = 2.0$ . At the lower Froude number,  $Fr_g = 1.0$ , de Leeuw's correlation predicts a slightly lower overread at lower  $X$  values ( $X < 0.15$ ). The data presented in this paper has more curvature at lower values of  $X$  than de Leeuw's data and correlation. The Steven correlation agrees better with the new data at lower values of  $X$  ( $X < 0.1$ ) as Steven's correlation has a similar initial gradient and curvature. However, at higher values of  $X$  Steven's correlation flattens off and predicts a significantly lower overreading. This is due to the fact that Stevens's data had a minimum pressure of 20 bar, and the correlation is in this case being used outside its original range. As the correlation was fitted using polynomials this is not advisable, as noted by Steven himself [6]. Fig. 18 shows the comparison for the  $\beta = 0.4$  Venturi at 60 bar. It can be seen that de Leeuw's correlation fits reasonably well again, particularly at the higher Froude number,  $Fr_g = 2.5$ . Once more, at the lower Froude number,  $Fr_g = 1.5$ , de Leeuw's correlation predicts a slightly lower overread at lower  $X$  values ( $X < 0.15$ ). The Steven correlation performs much better at 60 bar than it did at 15 bar. Again the Steven correlation matches the new data better at lower values of  $X$ . For the lower Froude number,  $Fr_g = 1.5$  Steven's correlation overpredicts slightly at  $X$  values between 0.1 and 0.25. At  $Fr_g = 2.5$  Steven's correlation fits very well up to  $X = 0.2$ , where it begins to underpredict.

Fig. 19 shows the comparison for the  $\beta = 0.75$  Venturi at 15 bar. It can be seen that de Leeuw's correlation does not match the new data very well for this meter. At  $Fr_g = 1.5$  de Leeuw's correlation again underpredicts at low  $X$  values ( $X < 0.1$ ) before crossing the new data and overpredicting at higher  $X$  values. At  $Fr_g = 3.5$ , de Leeuw's correlation predicts significantly higher overreadings than the new data shows. Steven's data shows the same trend as in the  $\beta = 0.4$  Venturi at 15 bar. Again, this is caused by using the correlation outside the range of its underlying data. Fig. 20 shows the comparison for the  $\beta = 0.75$  Venturi at 60 bar. de Leeuw's correlation shows the same trends with respect to the new data as in Fig. 19 at 15 bar, although the differences are smaller. Steven's correlation fits well again at lower values of  $X$  ( $X < 0.1$ ), but

above this value it begins to slightly overpredict the  $Fr_g = 1.5$  data and slightly underpredict the  $Fr_g = 4.5$  data.

Figs. 17 to 20 show graphically the shapes and trends of the two previous correlations and their comparison with the new data presented in this paper. For reasons of clarity, the information shown on these graphs is limited to a select few data sets. However, a fuller picture is given in Figs. 21 to 26.

Figs. 21 to 23 show the results of applying de Leeuw's correlation to the new data in terms of error in the corrected gas mass flowrate, at 15 bar, 30 bar and 60 bar respectively. Each graph shows the data for each of the three Venturis tested. At 15 bar de Leeuw's correlation corrects all the  $\beta = 0.4$  and  $\beta = 0.6$  data to within  $\pm 4\%$ . However, with the  $\beta = 0.75$  Venturi, de Leeuw's correlation significantly overcorrects the data from overreadings of 1.25 upwards. The same trends are apparent at 30 bar, although the magnitude of the over-correction for  $\beta = 0.75$  is reduced. At 60 bar, de Leeuw's correlation corrects almost all the data to within  $\pm 3\%$ , and all the  $\beta = 0.4$  and  $\beta = 0.6$  data to within 2%.

Is it clear that de Leeuw's correlation appears to fit the new data much better for the  $\beta = 0.4$  Venturi than the  $\beta = 0.75$  Venturi. It should be noted here that most of de Leeuw's data was collected using a 4-inch  $\beta = 0.4$  Venturi, and some with a 3-inch  $\beta = 0.4$  Venturi. As de Leeuw did not test any meters of a different  $\beta$  value it was not possible to include any  $\beta$  dependence in his correlation. However, de Leeuw [5] did state that, although different Venturi dimensions should be studied for their effect, these effects are expected to be minimal. This statement was based on previous work with orifice plates [7] which showed that  $\beta$  did not have a significant effect. The new data presented in this paper appears to show that the  $\beta$  value is very significant, and that the overreading decreases with increasing  $\beta$ .

Figs. 24 to 26 show the results of applying Steven's correlation to the new data in terms of error in the corrected gas mass flowrate, at 15 bar, 30 bar and 60 bar respectively. Each graph shows the data for each of the three Venturis tested. At 15 bar Steven's correlation corrects all the data up to an overreading of 1.3 to within  $\pm 5\%$ . However, above this value the error increases rapidly. As mentioned previously, this is caused by the fact that Steven's correlation is based on data from 20 bar to 60 bar and is a polynomial-based correlation. Use outside the original data range is not recommended. At 30 bar the performance is similar to that at 15 bar, with data up to an overreading of almost 1.35 predicted to within  $\pm 4\%$ , with larger errors at higher overreadings, although the magnitude of the errors is smaller. Again the principal reason for this fall off is that the correlation is being used outwith the original data range, as Steven's data did not feature as high values of  $X$  at 20 bar or 40 bar (the nearest pressures to the 30 bar tested here). At 60 bar, Steven's correlation predicts almost all the data to within  $\pm 4\%$  with the exception of a few high overreading points.

## 5 Future work

It is clear from the data presented here that the  $\beta$  value of a Venturi has a significant effect on the overreading in wet gas. Further analysis of the data presented here would be beneficial to developing a new Wet Gas Venturi correlation that takes into account gas pressure (density),  $Fr_g$ ,  $X$  and also  $\beta$ . Any development of such equation should also look at the performance outwith the original data set, with a view to ensuring stability when extrapolated.

Further work is currently planned at NEL to investigate the performance of Wet Gas Venturis using different fluids. It is expected that this data will further improve the understanding of the behaviour of Venturis in wet gas flows and also of the key parameters that affect this behaviour.



## 6 Conclusions

Three Venturi meters have been tested in Wet Gas in NEL's Wet Gas Test Facility. The meters, with  $\beta$  values of 0.4, 0.6 and 0.75 have been tested at 15 bar, 30 bar and 60 bar across a range of gas Froude numbers,  $Fr_g$ , and Lockhart-Martinelli values,  $X$ . The results confirm that the gas pressure (density) has a significant effect on the meter overreading, with the overreading decreasing with increasing pressure. The results also confirmed that the gas velocity, or  $Fr_g$ , has a significant effect on the overreading, with the overreading increasing with increasing gas velocity, or  $Fr_g$ . The new data is the first to show results from Venturis with different  $\beta$  values, and in fact show that the  $\beta$  value has a significant effect on the meter overreading.

Analysis of the existing wet gas Venturi correlations shows that further work is required to accommodate the new data presented here, taking into account the  $\beta$  value. Care should be taken when applying any of the existing correction factors to ensure that they are not used in situations where the key parameters noted above,  $Fr_g$ ,  $X$ ,  $\beta$ , etc are outwith the range used to develop the correlation.

## 7 Nomenclature

|                   |   |  |
|-------------------|---|--|
| $m_{g(actual)}$   | = | corrected gas mass flowrate, [kg/s]                      |
| $m_{g(tp)}$       | = | apparent gas mass flowrate, [kg/s]                       |
| $X$               | = | "modified" Lockhart-Martinelli parameter, [ - ]          |
| $m_g$             | = | gas mass flowrate, [kg/s]                                |
| $m_l$             | = | liquid mass flowrate, [kg/s]                             |
| $\rho_g$          | = | gas density, [kg/m <sup>3</sup> ]                        |
| $\rho_l$          | = | liquid density, [kg/m <sup>3</sup> ]                     |
| $C$               | = | Venturi discharge coefficient, [ - ]                     |
| $E$               | = | velocity of approach factor, [ - ]                       |
| $\varepsilon$     | = | gas expansibility, [ - ]                                 |
| $A_d$             | = | Venturi throat area, [m <sup>2</sup> ]                   |
| $\Delta p_{(tp)}$ | = | measured two-phase differential pressure, [bar]          |
| $\beta$           | = | ratio of pipe diameter to Venturi throat diameter, [ - ] |
| $Fr_g$            | = | gas Froude number, [ - ]                                 |
| $V_{sg}$          | = | superficial gas velocity, [m/s]                          |
| $g$               | = | gravitational constant, [m/s <sup>2</sup> ]              |
| $D$               | = | pipe diameter, [ - ]                                     |
| $\Delta p_{(g)}$  | = | estimated gas differential pressure, [bar]               |
| $m_{g(ref)}$      | = | dry gas reference mass flowrate, [kg/s]                  |
| $K_g$             | = | dry gas flow coefficient, [ - ]                          |
| $Re_{g,ref}$      | = | reference gas Reynolds number, [ - ]                     |

## Acknowledgments

The work described in this paper was carried out as part of the 1999 – 2002 Flow Programme, funded by the UK Department of Trade and Industry's National Measurement Systems Directorate.

## References

- [1] Murdock, J.W.: "Two-Phase Flow Measurement with Orifices", *Journal of Basic Engineering* (1962) pp. 419-433.
- [2] Chisholm, D.: "Flow of Incompressible Two-Phase Mixtures through Sharp-Edged Orifices", *Journal of Mechanical Engineering Science* (1967) 9, No. 1.
- [3] Chisholm, D.: "Research Note: Two-Phase Flow through Sharp-Edged Orifices", *Journal of Mechanical Engineering Science* (1977) 19, No. 3.
- [4] Lin, Z.H.: "Two-Phase Flow Measurements with Sharp-Edged Orifices", *International Journal of Multiphase Flow* (1982) 8, No. 6, pp. 683.
- [5] de Leeuw, R.: "Liquid Correction of Venturi Meter Readings in Wet Gas Flow", Paper 21 presented at the 1997 North Sea Flow Measurement Workshop, Gleneagles Hotel, Scotland, October 24-27.
- [6] Steven, R.: "Wet Gas Metering", Ph.D. Thesis at University of Strathclyde, Glasgow, Scotland, UK, April 2001.
- [7] Mattar, L., Aziz, K., and Gregory, G., "Orifice metering of two phase flow", SPE Paper 7411, October 1978.

Figures

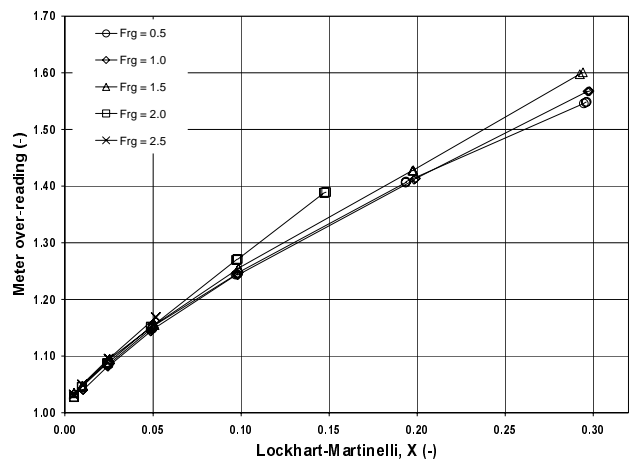


Fig. 1. Overreading for  $\beta = 0.4$  Venturi at 15 bar.

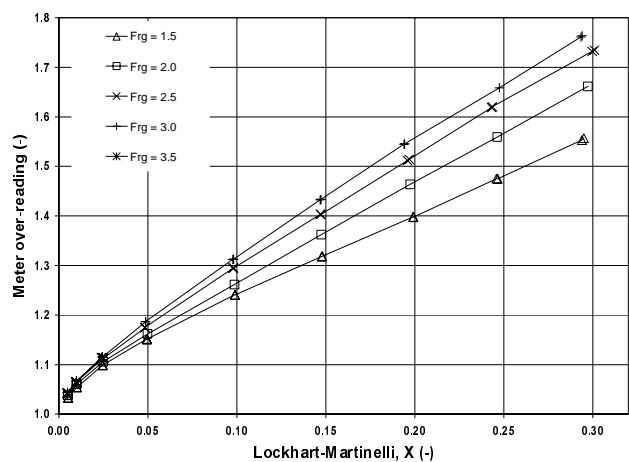


Fig. 4. Overreading for  $\beta = 0.6$  Venturi at 15 bar.

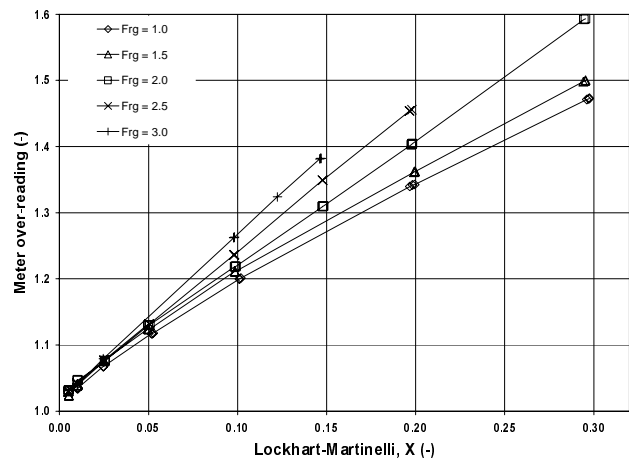


Fig. 2. Overreading for  $\beta = 0.4$  Venturi at 30 bar.

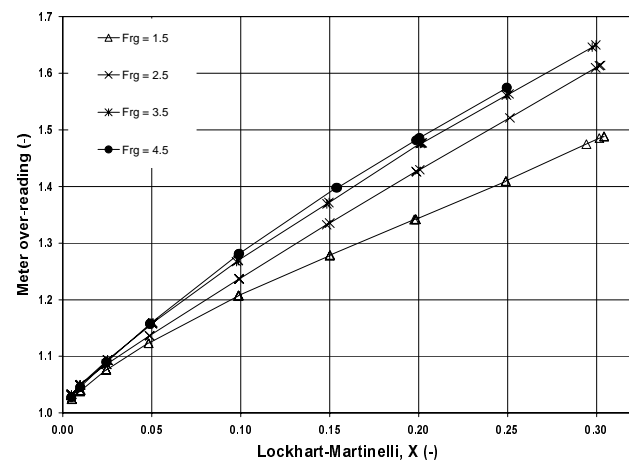


Fig. 5. Overreading for  $\beta = 0.6$  Venturi at 30 bar.

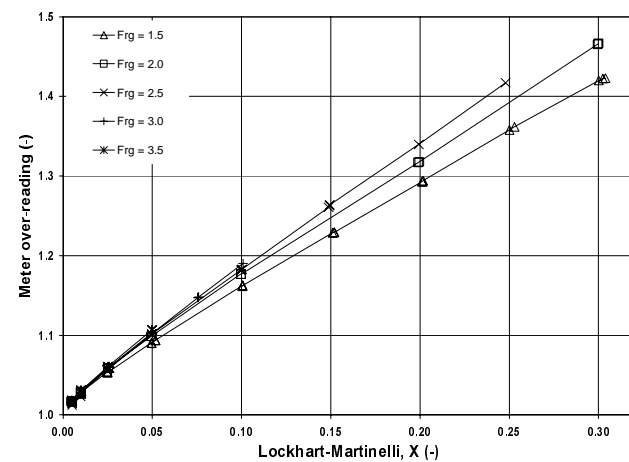


Fig. 3. Overreading for  $\beta = 0.4$  Venturi at 60 bar.

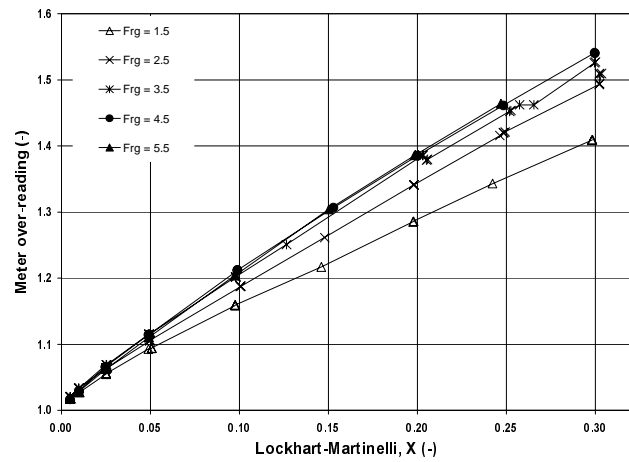


Fig. 6. Overreading for  $\beta = 0.6$  Venturi at 60 bar.

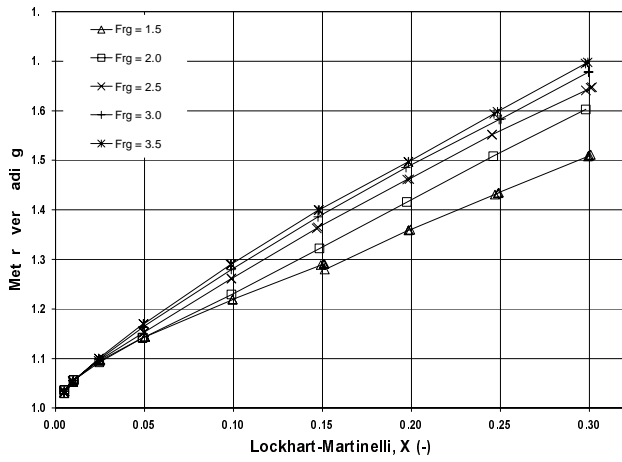


Fig. 7. Overreading for  $\beta = 0.75$  Venturi at 15 bar.

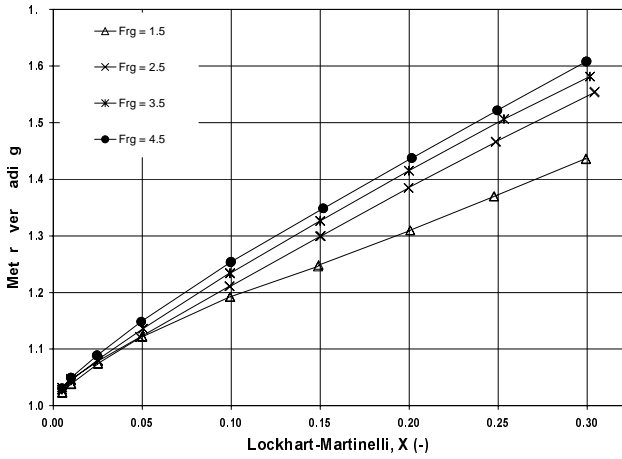


Fig. 8. Overreading for  $\beta = 0.75$  Venturi at 30 bar.

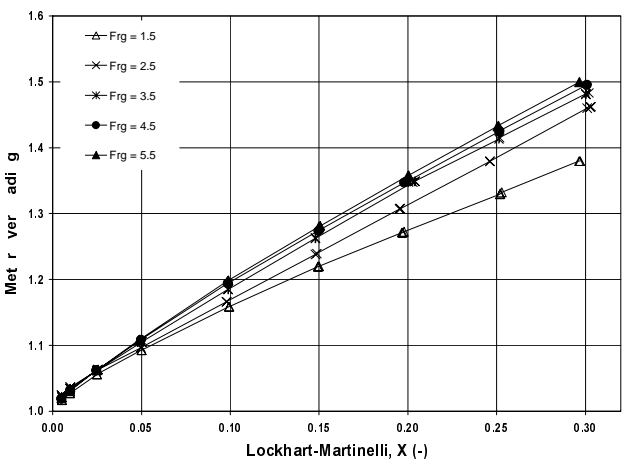


Fig. 9. Overreading for  $\beta = 0.75$  Venturi at 60 bar.

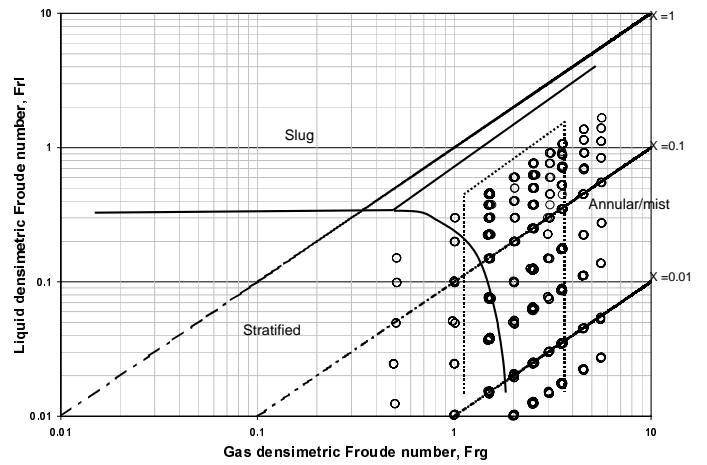


Fig. 10. Reproduction (from [4]) of a Shell flow pattern map showing NEL test data and de Leeuw [4] test envelope (dotted).

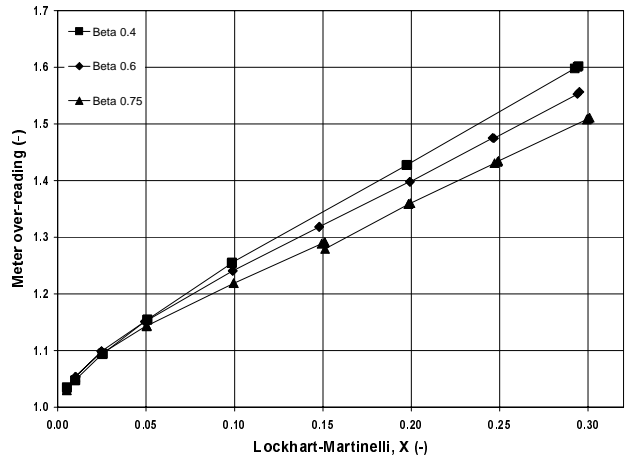


Fig. 11. Overreading at 15 bar and  $Fr_g = 1.5$ , at different  $\beta$  values.

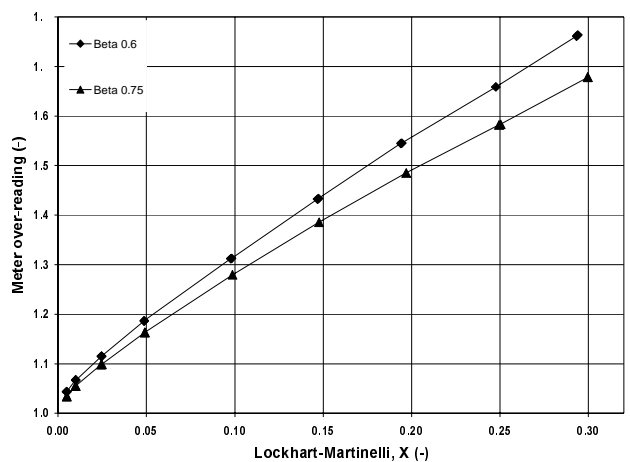


Fig. 12. Overreading at 15 bar and  $Fr_g = 3.0$ , at different  $\beta$  values.

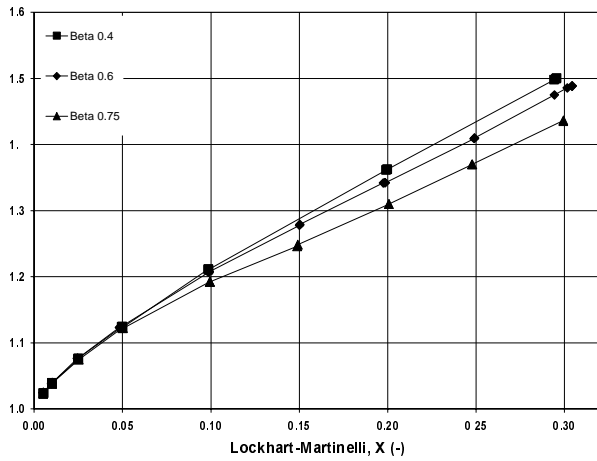


Fig. 13. Overreading at 30 bar and  $Fr_g = 1.5$ , at different  $\beta$  values.

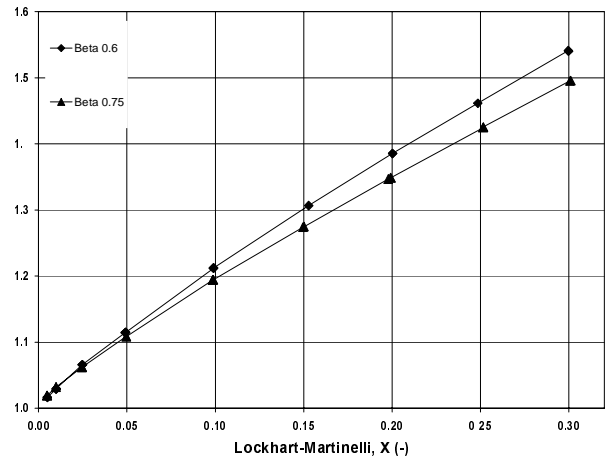


Fig. 16. Overreading at 60 bar and  $Fr_g = 4.5$ , at different  $\beta$  values.

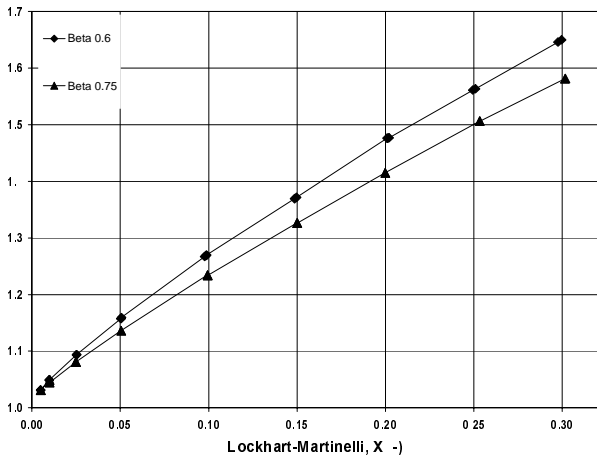


Fig. 14. Overreading at 30 bar and  $Fr_g = 3.5$ , at different  $\beta$  values.

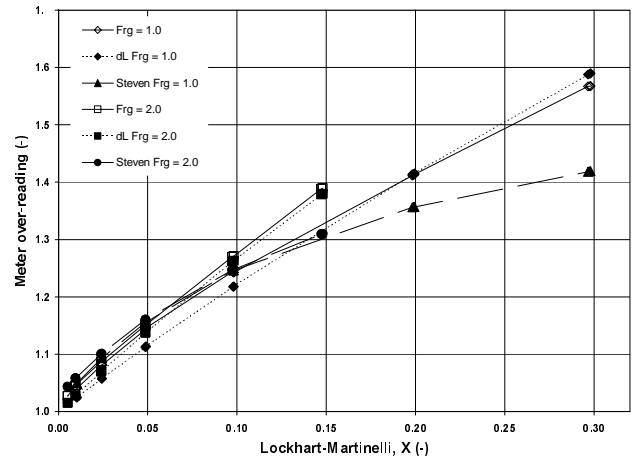


Fig. 17. Comparison of de Leeuw and Steven correlations with  $\beta = 0.4$  at 15 bar.

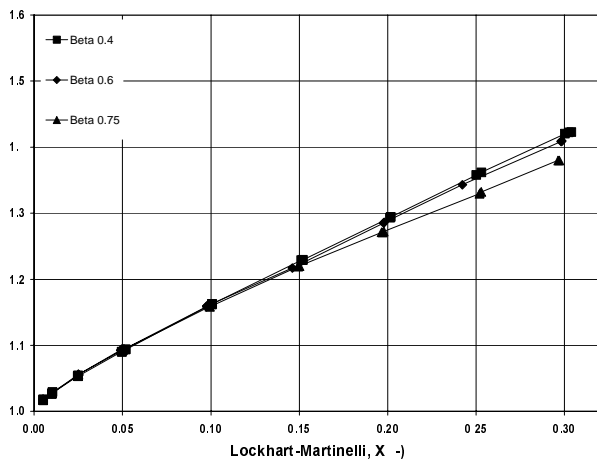


Fig. 15. Overreading at 60 bar and  $Fr_g = 1.5$ , at different  $\beta$  values.

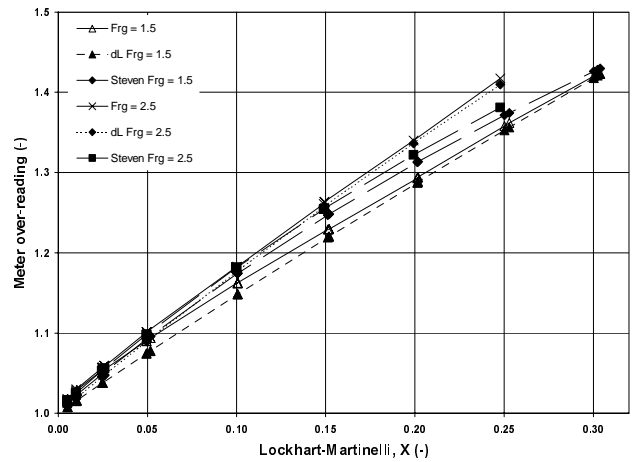


Fig. 18. Comparison of de Leeuw and Steven correlations with  $\beta = 0.4$  at 60 bar.

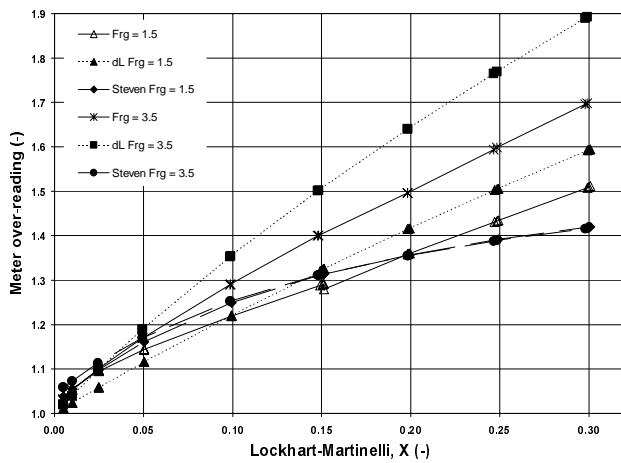


Fig. 19. Comparison of de Leeuw and Steven correlations with  $\beta = 0.75$  at 15 bar.

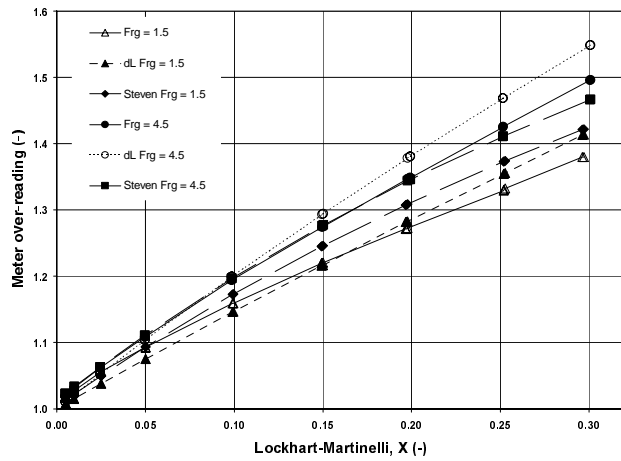


Fig. 20. Comparison of de Leeuw and Steven correlations with  $\beta = 0.75$  at 60 bar.

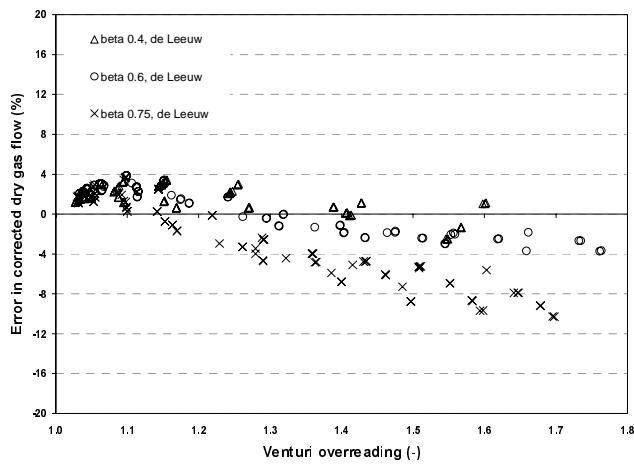


Fig. 21. Comparison of corrected dry gas flow using de Leeuw correlation at 15 bar.

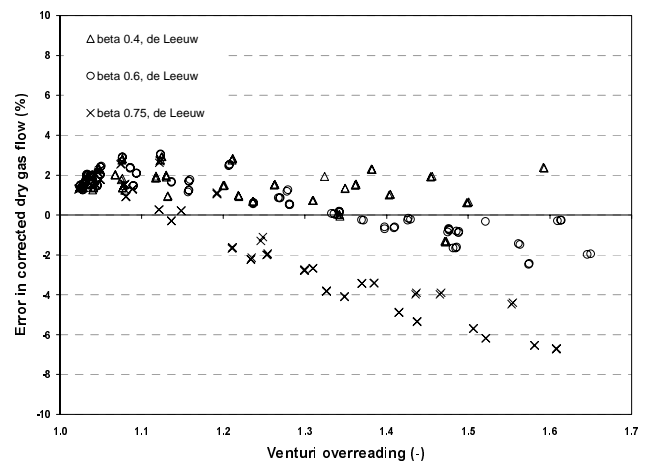


Fig. 22. Comparison of corrected dry gas flow using de Leeuw correlation at 30 bar.

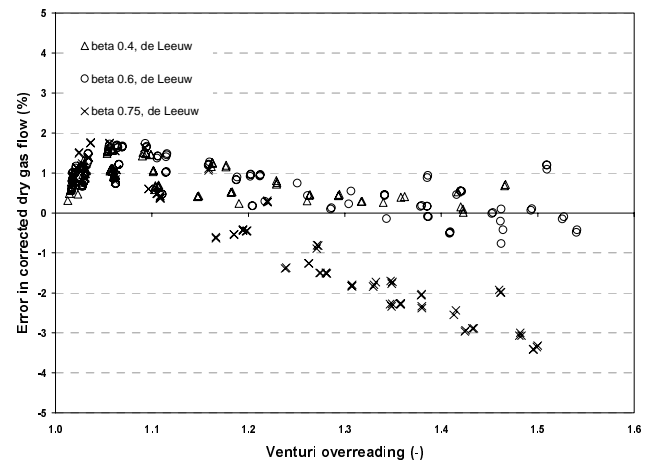


Fig. 23. Comparison of corrected dry gas flow using de Leeuw correlation at 60 bar.

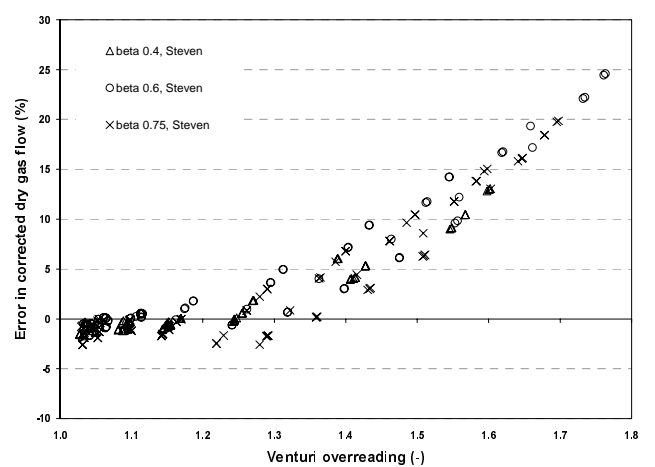


Fig. 24. Comparison of corrected dry gas flow using Steven correlation at 15 bar.

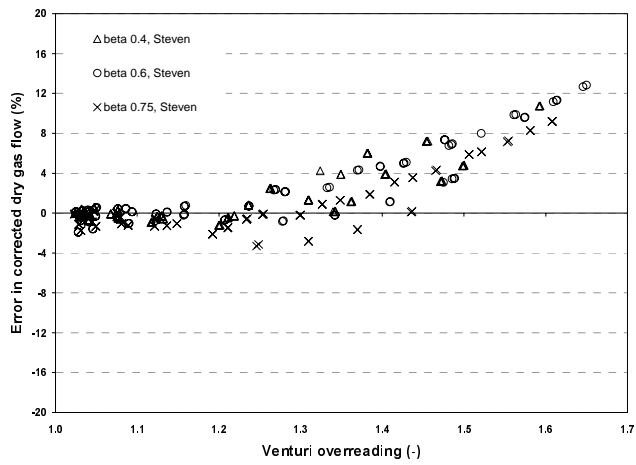


Fig. 25. Comparison of corrected dry gas flow using Steven correlation at 30 bar.

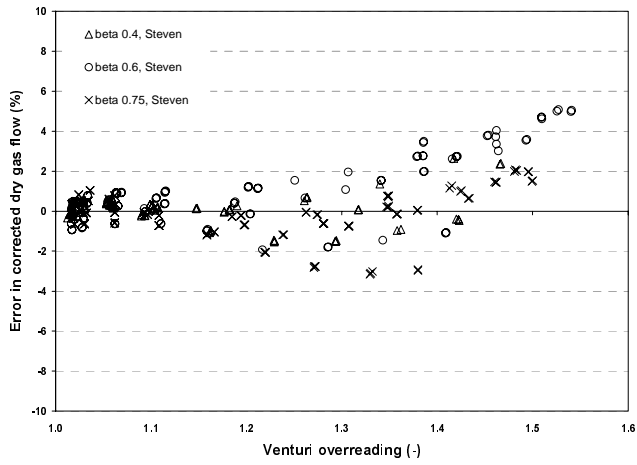


Fig. 26. Comparison of corrected dry gas flow using Steven correlation at 60 bar.

